IJRCS

International Journal of Robotics and Control Systems
Vol. 5, No. 5, 2025, pp. 2653-2668
ISSN 2775-2658
http://pubs2.ascee.org/index.php/ijrcs

ASCEE

Thermo-Mechanical Modeling and Iterative Learning Control for Electrothermal Microgrippers with Integrated Compliant Rotary Joints

Dzung Tien Nguyen [a,1,*], Duc Minh Ngo [a,2]

[a] Thai Nguyen University of Technology, Thai Nguyen 250000, Vietnam
[1] dungnguyentien@tnut.edu.vn; [2] ngoduc198-tdh@tnut.edu.vn
* Corresponding Author

ARTICLE INFO

Article history
Received August 18, 2025
Revised September 20, 2025
Accepted November 24, 2025

Keywords
V-Shaped Electrothermal;
Actuators;
Microgripper;
Compliant Rotary Joint;
Thermo-Mechanical Modeling;
Iterative Learning Control (ILC);
PID-Proportional Integral Derivative;
PD-Proportional Derivative

ABSTRACT

This study presents the modeling, control design, and simulation of a MEMS-based V-shaped electrothermal microgripper integrated with compliant rotary joints as a novel mechanical enhancement to achieve both displacement amplification and stress reduction. A comprehensive thermo–mechanical model was developed, including heat conduction, thermo-elastic deformation, and kinematic transmission; the modeling assumptions are explicitly stated (neglecting convection and radiation, assuming small angular deflections), yielding an amplification ratio of approximately 3.33. The main contributions include developing a tractable thermo-mechanical model, integrating compliant rotary joints, and evaluating PD/PID-ILC for high-precision trajectory tracking. Two iterative learning control (ILC) schemes, namely PD-ILC and PID-ILC, were implemented in MATLAB/Simulink for trajectory tracking of a trapezoidal reference signal with a peak jaw displacement of 40 µm. Simulation results show that both controllers achieve convergence within finite iterations, with PID-ILC exhibiting faster convergence and smaller tracking errors. The steady-state error was about 0.21 µm (0.52% of 40 µm), while the maximum post-convergence error was 1.73 µm (4.33%). The results highlight the advantages of iterative learning control, which can progressively reduce tracking errors over repeated tasks while maintaining a simple structure suitable for MEMS implementation. These findings confirm the effectiveness of the proposed control strategies in compensating for thermal delays and nonlinearities, enabling high-precision micromanipulation in biomedical handling, micro-assembly, and precision optics. Nevertheless, this paper acknowledges its limitations (lack of experimental validation and sensitivity to parameter variations) and outlines future research directions, including real-time implementation, robustness testing under disturbances, and the development of adaptive ILC variants.

1. Introduction

Microgrippers are indispensable tools in micromanipulation and micro/nano-assembly, functioning as end-effectors for handling microscale objects in domains such as microsurgery, cellular

biology, micro-assembly, and precision instrumentation [1]-[6]. Their integration in micro-opto-electro-mechanical systems (MOEMS) has enabled significant advances in applications ranging from Fourier-transform microspectrometers to multi-degree-of-freedom microrobots [7]-[10].

A generic microgripper is typically composed of three subsystems: (i) an actuator that provides the driving force, (ii) a motion amplification or compliant transmission mechanism, and (iii) gripping jaws in contact with the target object [11]-[14]. Among these, the actuator decisively determines gripping force, displacement, and dynamic response. Reported actuation techniques include electrostatic, piezoelectric, electromagnetic, shape memory alloy (SMA), electrothermal, and vacuum-driven actuators [15]-[18]. Within this landscape, electrothermal V-shaped actuators have attracted particular interest due to their large output force, low-voltage operation, and MEMS-compatible fabrication [19]-[23].

To improve displacement efficiency and reliability, recent studies have focused on dimension optimization [24]-[26], stress reduction via compliant mechanisms [29]-[32], material surface engineering such as platinum sputtering for reduced resistance [33], and self-locking mechanisms for energy-efficient holding [21], [22]. These advances underscore the importance of integrating mechanical design innovations with multiphysics modeling to fully exploit the potential of MEMS-based grippers [34]-[36].

In parallel with mechanical optimization, control strategies have become a research frontier. Open-loop actuation often suffers from nonlinear thermal dynamics, hysteresis, and parameter uncertainties [37]-[39]. To address these challenges, diverse closed-loop and learning-based methods have been introduced. Proportional–integral–derivative (PID) control remains the most widely used for displacement tracking due to its simplicity and real-time feasibility [40]-[43]. Adaptive and robust control approaches such as sliding mode, H∞, and disturbance observer–based strategies further improve resilience to uncertainties [44]-[47]. Model predictive control (MPC) has been adopted to compensate for thermal lag and operational constraints, yielding improved transient performance [48], [49].

Among advanced techniques, Iterative Learning Control (ILC) is particularly suited for repetitive micromanipulation, progressively reducing trajectory-tracking error over iterations [26], [50]-[53]. Extensions such as PD-type and PID-type ILC have demonstrated superior convergence and robustness in MEMS actuators [27], [28], [51], [52]. Hybrid approaches that combine ILC with feedforward compensation or intelligent schemes (e.g., fuzzy logic or neural networks) have also been reported to enhance adaptability in uncertain environments [54]-[60].

Nevertheless, existing studies still exhibit several limitations. Most works have emphasized either mechanical optimization or control design in isolation, with relatively limited efforts toward integrating detailed thermo-mechanical modeling, compliant mechanism innovations, and advanced control. Furthermore, experimental validation and systematic robustness analysis remain sparse, leaving an important gap between simulation-level results and practical micromanipulation requirements.

To address these challenges, this paper presents a V-shaped electrothermal microgripper with integrated compliant rotary joints, designed to simultaneously reduce stress concentrations and enhance displacement amplification. A comprehensive thermo-mechanical model is developed, explicitly stating the assumptions (neglecting convection and radiation, assuming small angular deflections), and two iterative learning control (ILC) strategies-PD-ILC and PID-ILC-are implemented in MATLAB/Simulink to evaluate precision trajectory tracking.

The main contributions are threefold: (i) development of an analytically tractable thermo-mechanical model tailored for control design; (ii) structural integration of compliant rotary joints for improved performance; and (iii) systematic evaluation of PD-ILC and PID-ILC, highlighting the advantages of ILC in progressively reducing errors while maintaining simplicity for MEMS implementation. This integrated approach targets biomedical micromanipulation, micro-assembly, and intelligent robotic systems, where high precision, repeatability, and operational safety are critical.

2. Configuration and Working Principles

2.1. Configuration

The proposed electrothermal microgripper consists of nine main components (1–9) (Fig. 1), arranged symmetrically to achieve high-precision actuation in microscale environments. The gripper jaws (1) are mounted on two gripper arms (2), which rotate around compliant pivot points formed by elastic bars (3). These bars are fixed to the anchor base (4), ensuring structural stability and providing restoring force after actuation.

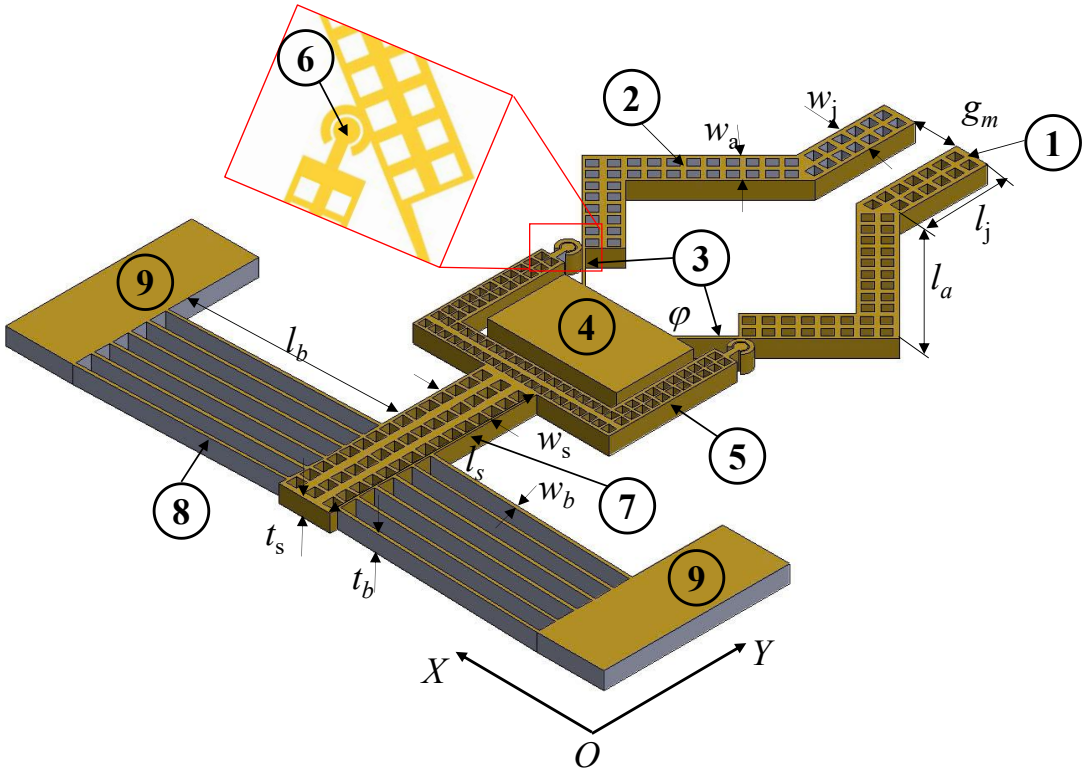

Fig. 1. The configuration of microgripper

Motion is transmitted to the gripper arms via a central U-shaped link claw (5), connected to a central shuttle (7). This shuttle moves vertically in the Y-direction and is linked to the arms through soft revolute joints (6), which enhance displacement amplification while minimizing stress concentration. The shuttle is actuated by a pair of V-shaped thermal beams (8), arranged symmetrically and fabricated using MEMS-compatible processes. Heating these beams via electrodes (9) causes thermal expansion, driving the shuttle upward. This motion is then transferred through the mechanical linkage to close the gripper jaws. The entire system is monolithically fabricated from silicon, optimized for low driving voltage, compactness, and integration with SOI-MEMS technology. The design enables reliable, energy-efficient, and repeatable micro-manipulation, making it suitable for biomedical, microrobotics, and precision assembly applications.

A key novelty of the proposed design lies in the integration of compliant rotary joints within the transmission mechanism. Unlike conventional rigid pivots, these joints are realized by flexure hinges that allow smooth rotational motion without introducing mechanical backlash. Their compliant nature not only facilitates displacement amplification from the shuttle to the jaws but also redistributes stress concentrations away from critical junctions, thereby improving structural reliability and fatigue resistance. This integration eliminates the need for complex hinge fabrication or assembly, ensuring full MEMS compatibility and monolithic realization. By combining displacement amplification and stress mitigation in a single structural feature, the compliant rotary joints significantly enhance both the performance and durability of the microgripper, making it particularly well-suited for repetitive biomedical and micromanipulation tasks.

2.2. Working Principle

When an electrical voltage is applied across the electrodes (9), current flows through the V-shaped beams (8), generating heat via Joule heating. This thermal energy induces expansion in the inclined beams, producing a net force that displaces the shuttle (7) upward along the Y-axis.

The vertical motion of the shuttle is transmitted through the U-shaped claw (5), which pushes both gripper arms (2) symmetrically via the revolute joints (6). These joints convert the linear displacement into rotational motion around the compliant point O, formed by the elastic bars (3). As a result, the gripper jaws (1) at the distal ends of the arms move toward each other to grasp the target object. When the voltage is removed, the V-beams cool down and contract, while the elastic restoring force from the elastic bars (3) brings the system back to its initial open configuration. This cycle enables repeatable micro-gripping operations with high precision and minimal energy input, making the microgripper suitable for tasks such as cell manipulation, micro-assembly, and lab-on-a-chip systems.

3. Mathematical Modeling of the Electrothermal Microgripper

To accurately describe the operation of a microgripper actuated by V-shaped electrothermal actuators, we construct a coupled multiphysics model comprising three domains: thermal, electrical, and mechanical. This model includes: (1) heat generation and temperature distribution along the actuator beams; (2) thermal expansion and displacement of the central slider, and (3) mechanical transmission from the slider to the gripping jaws via soft rotary joints.

3.1. Electro-Thermal Model of the V-Shaped Beam

During operation, the temperature in V-shaped beams system is not uniformly distributed. In this case, we assume that convection and radiant heat transfer are ignored; temperature is distributed along the V-shaped beam length (x-direction). At the bond pads (9) the temperature is room temperature, near the shuttle (7) the temperature will be highest. The heat transfer model can be written in either a finite difference [17], [23] or an analytical form. The beam is splitted into many small elements with an assumption that elements are supposed to be homogeneous and the heat source is evenly distributed on those elements. Structure of the V-shaped electrothermal microactuator (VEM) shown in Fig. 2. Consider the heat transfer process in an equivalent beam of length$2l_b$ (Fig. 3).

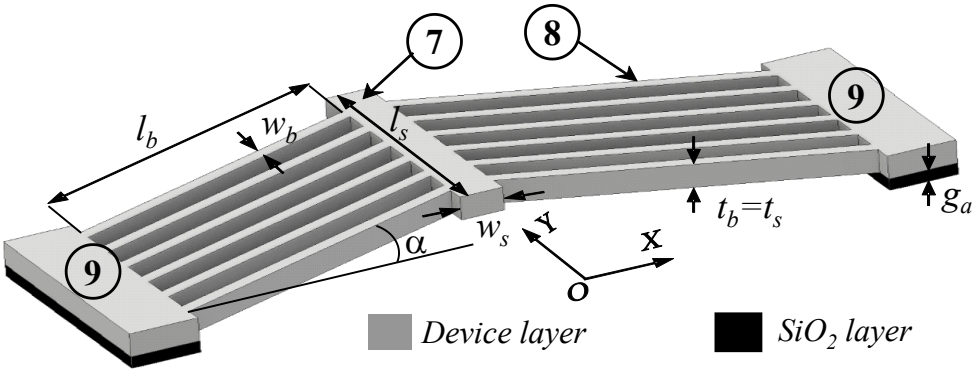

Fig. 2. Structure of the V-shaped electrothermal microactuator (VEM)

To keep the mathematical formulation analytically tractable, several simplified assumptions were introduced. In particular, heat transfer by convection and radiation was neglected, and small angular deflections were assumed in the compliant rotary joints. Such assumptions reduce the complexity of the coupled thermo–mechanical model and make the controller design more computationally efficient. This is justified by the fact that Iterative Learning Control (ILC) does not rely on a highly accurate plant model, since controller parameters can be progressively tuned through repeated trials and adjustments across iterations. Nevertheless, the implications of these assumptions are further discussed in next section. Then, at a very small element of length dx on a beam whose coordinate position is x, the heat balance equation is given as follows:

$$q_{st} = q_{cd} + q_{ls} + q_e \tag{1}$$

Where q_{st} is heat energy stored in beam element; q_{cd} is the heat transfer through the beam element; q_{ls} is the heat transferred from the beam element to the foundation through the air gap g_a; q_e is the heat generated in the beam element when an electric current is passed.

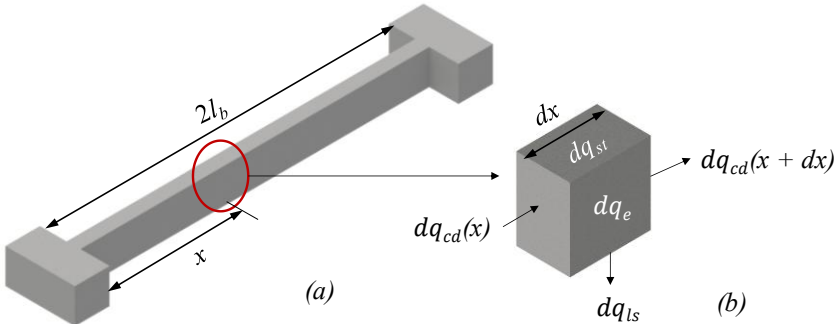

Fig. 3. General line-shaped model of V-shaped

In which:

$$q_{st} = C_p.d\frac{dT}{dt}.A.dx;\ q_{cd} = k_s.A.\frac{\partial T}{\partial x}\Big|_{x+dx} - k.A.\frac{\partial T}{\partial x}\Big|_x;\ q_{ls} = -\frac{k_a.S}{g_a}.(T-T_0).w.dx;$$
$$q_e = \frac{V^2}{4\rho.L^2}.A.dx \tag{2}$$

Where, C_p,d,k_s are specific heat, density and thermal conductivity of silicon material; k_a,$g_a$are thermal conductivity of air and air gap between beam and substrate; S is the shape factor of beam area section: $S = 0.6265\left(\frac{t_b}{w_b}\right) + 1.1188$ (determined by simulation); $A = t_b.w_b$ is the cross-section area of beam; $T$and $T_0$are the temperature of beam element and environment temperature; $t$is time; V is the driving voltage; ρ is resistivity of silicon. Substitute (2) into (1), we have the heat transfer differential equation (3).

$$C_p.d.\frac{dT}{dt} = k_s.\frac{\partial^2 T}{\partial x^2} - \frac{k_a.S}{t_b.g_a}(T-T_0) + \frac{V^2}{4\rho.l_b^2} \tag{3}$$

We find that the temperature distribution depends on time (t) and space (ox). Using the variable decomposition method, Equation (3) has a solution (4):

$$T(x,t) = T_0 + q_e.\frac{t_b.g_a}{k_a S}(1 + C_1.e^{\tau x} + C_2.e^{-\tau x}) + \sum_{r=1}^{\infty} B_r.e^{-[\gamma.\lambda_r^2+\beta].t}.sin(\lambda_r.x) \tag{4}$$

In which: B_r is determined from the initial condition $T(x,t=0) = T_0$.

$$B_r = 2q_e.\frac{t_b.g_a}{k_a.S}.\left[\frac{4\tau^2.l_b^2}{r.\pi.(4\tau^2.l_b^2 + r^2.\pi^2)}\right].[cos(r.\pi) - 1] \tag{5}$$

C_1, C_2, λ_r are determined from the boundary condition $T(x=0,t) = T(x=2l_b,t) = T_0$.

$$C_1 = q_e.\frac{t_b.g_a}{k_a.S}.\frac{(e^{-2\tau.l_b}-1)}{(e^{2\tau.l_b}-e^{-2\tau.l_b})};\ C_2 = -q_e.\frac{t_b.g_a}{k_a.S}.\frac{(e^{2\tau.l_b}-1)}{(e^{2\tau.l_b}-e^{-2\tau.l_b})};\ \lambda_r = \frac{r.\pi}{2l_b} \tag{6}$$

r is the number of orders of the temperature solution (T), usually we choose $r = 1$; $\gamma$and β are coefficients calculated according to the formulas:

$$\gamma = \frac{k_s}{C.d};\ \beta = \frac{k_a.S}{t_b.g_a.C.d} \tag{7}$$

3.2. Thermal Expansion Force

When an electric current is passed the V-beams, which will be heated and expanded along the beam length. This expansion produces force and displacement, which have been calculated in detail in [19], [20], [26]. Thermal expansion force acting on the shuttle shown in Fig. 4.

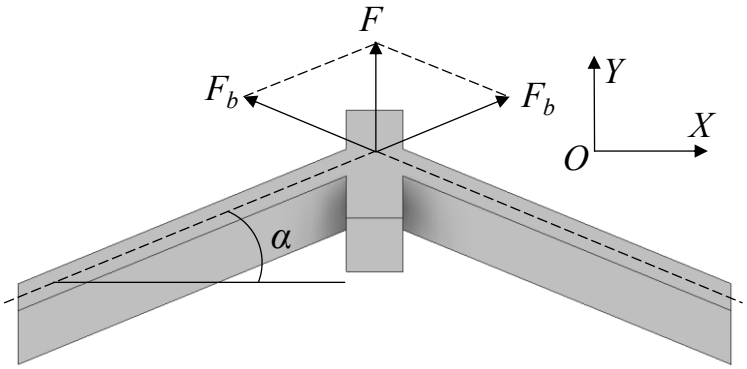

Fig. 4. Thermal expansion force acting on the shuttle

The total thermal expansion force of V-shaped beam system acting on the shuttle in Y-direction is expressed as.

$$F = 2n.F_b.\sin\alpha = 2n.A.E.\frac{\Delta l_b}{l_b}.\sin\alpha \tag{8}$$

Where: F_b is thermal expansion force generates along the single beam; Δl_b is total thermal expansion along the length l_b of the single beam α_l is a thermal expansion coefficient of silicon; $E = 1.69 \times 10^5$ (MPa) is the Young's modulus of silicon.

$$F_b = A.E.\frac{\Delta l_b}{l_b} \tag{9}$$

$$\Delta l = \sum_i \alpha_l.(T_i - T_0)..\Delta x \tag{10}$$

According to [26], The vertical displacement (i.e., in the y-direction) of the single beam can be calculated as:

$$\Delta d_i = \sqrt{(l_b + \Delta l_b)^2 - (l_b cos\,\alpha)^2} - l_b\,sin \tag{11}$$

The displacement of the actuator system Δd equals the vertical displacement of a single beam plus a half of the expansion of the shuttle $\frac{1}{2}\Delta l_s$ (assuming that the shuttle expands on both tips B). We have:

$$\Delta d = \sqrt{(l_b + \Delta l_b)^2 - (l_b cos\,\alpha)^2} - l_b \sin\alpha + \frac{1}{2}\Delta l_s \tag{12}$$

3.3. Kinematic Model of Gripper Jaw Displacement

The slider transmits displacement through a U-shaped frame to the soft rotary joint at point O. This segment is modeled as a rotational lever system, where the linear input displacement δ_y is transformed into a small rotational angle θ_g of each jaw, approximated as:

$$\theta_g \approx \frac{\Delta d}{d} \tag{13}$$

where d is the distance from the slider to the rotation point O. The tip displacement of each jaw is:

$$\delta_g = L.\theta_g = \frac{L}{d}\Delta d = \frac{L}{d}\left(\sqrt{(l_b + \Delta l_b)^2 - (l_b \cos\alpha)^2} - l_b \sin\alpha + \frac{1}{2}\Delta l_s\right) \quad (14)$$

L represents the distance from the rotation point O to the tip of each gripper jaw — i.e., the effective lever arm length of the gripper arm. Therefore, the total opening gap between the two jaws becomes:

$$g(V) = 2\delta_g = \frac{2L}{d}\Delta d = \frac{2L}{d}\left(\sqrt{(l_b + \Delta l_b)^2 - (l_b \cos\alpha)^2} - l_b \sin\alpha + \frac{1}{2}\Delta l_s\right) \quad (15)$$

3.4. Dynamic Model and Iterative Learning Control (ILC)

Given the repetitive nature of micrograpping tasks, the system dynamics of the microgripper can be modeled as a discrete-time nonlinear system, where the control input is the driving voltage $u_k(t)$, the system output is the gripper jaw displacement $y_k(t)$:

$$x_{k+1}(t+1) = f\{x_k(t), u_k(t)\}, y_k(t) = h\{x_k(t)\} \quad (16)$$

To track a predefined reference trajectory $r_k(t)$, we adopt an Iterative Learning Control (ILC) approach, which updates the control input across iterations based on the tracking error history:

$$u_{k+1}(t) = u_k(t) + K.e_k(t) \text{ với } e_k(t) = r(t) - y_k(t) \quad (17)$$

Trong đó: where: K is learning gain, $e_k(t)$ is tracking error at the k^{th} iteration. To enhance convergence speed and control robustness, especially in the presence of nonlinearities and thermal delays inherent in electrothermal actuators, the ILC update rule is extended to incorporate PD or PID-type learning [26], [47], [52]:

$$\text{(a) PD-type ILC update: } u_{k+1}(t) = u_k(t) + K_P e_k(t) + K_D e_k(t+1) \quad (18)$$

$$\text{(b) PID-type ILC update: } u_{k+1}(t) = u_k(t) + K_P e_k(t) + K_I e_k(t-1) + K_D e_k(t+1) \quad (19)$$

In these formulations K_P, K_I, K_D : proportional, integral, and derivative learning gains, respectively; The integral term accumulates past errors to reduce steady-state deviation; The derivative term anticipates future errors, improving response to dynamic changes.

This enhanced ILC framework improves convergence rate, mitigates overshoot, and compensates for time delays due to thermal inertia, thereby yielding more accurate and stable control of jaw displacement in cyclic micromanipulation tasks.

4. Simulation and Performance Evaluation

To evaluate the behavior and control performance of the proposed electrothermal microgripper, numerical simulations were conducted directly based on the mathematical model established in Section 3. The entire simulation framework was developed using MATLAB/Simulink, incorporating the coupled electro-thermal-mechanical dynamics and iterative learning-based control laws.

Using the geometric parameters of the microgripper provided in Table 1, the material properties in Table 2, and the single-jaw displacement mathematical model in equation (14), simulations were carried out employing the PD iterative learning algorithm in equation (18) and the PID iterative learning algorithm in equation (19). The control gains were preliminarily selected based on initial conditions to ensure system stability and convergence. In this study, the chosen values were $K_P = 0.16; K_I = 0.2; K_D = 0.2$. The reference signal was assumed to have a trapezoidal waveform with an amplitude of δ_{max}. The simulation results are presented in the corresponding Fig. 5, Fig. 6, Fig. 7, Fig. 8, Fig. 9, Fig. 10.

From the iterative learning simulation results, it can be observed that the system error decreases after each learning iteration, indicating that the system satisfies the convergence condition within a

finite number of iterations. Once the "convergence" iteration number was determined, simulations were performed, and the results are illustrated in Fig. 5 and Fig. 6. These results show that the output signal tracks the reference relatively well, with an average sum of squared errors (Norm) of 9.24 for the PD learning algorithm and 5.47 for the PID learning algorithm. In the steady-state operating region, the tracking error is about 0.23 μm, which corresponds to approximately 0.58% for PD (165 iterations) and 0.52% for PID (105 iterations), relative to the reference amplitude of 40 μm. This indicates that the system exhibits a relatively small steady-state error. In the "slope" regions of the operating cycle, the error is higher, with the maximum error reaching 1.97 μm (approximately 4.93% for PD and 4.33% for PID relative to the reference amplitude).

Table 1. Geometric parameters of the microgripper

Parameters	Symbol	Unit	Value
The length of gripper jaw (1)	l_j	μm	170
The width of gripper jaw (1)	w_j	μm	60
Maximum displacement of gripper jaws	g_m	μm	80
The length of gripper arm (2)	l_a	μm	300
The width of gripper arm (2)	w_a	μm	60
The length of central shuttle (7)	l_s	μm	350
The width of central shuttle (7)	w_s	μm	100
Number of V-beam pairs	n	$pair$	10
The length of a single V-beam (8)	l_b	μm	700
The width of a single V-beam (8)	w_b	μm	6
The thickness of a single V-beam (device layer)	$t_b = t_s$	μm	30
The incline angle of V-beam to the x-direction	θ	°	2
The incline angle of elastic bars to the y-direction	φ	°	45
Air gap between beam and substrate	g_a	μm	4

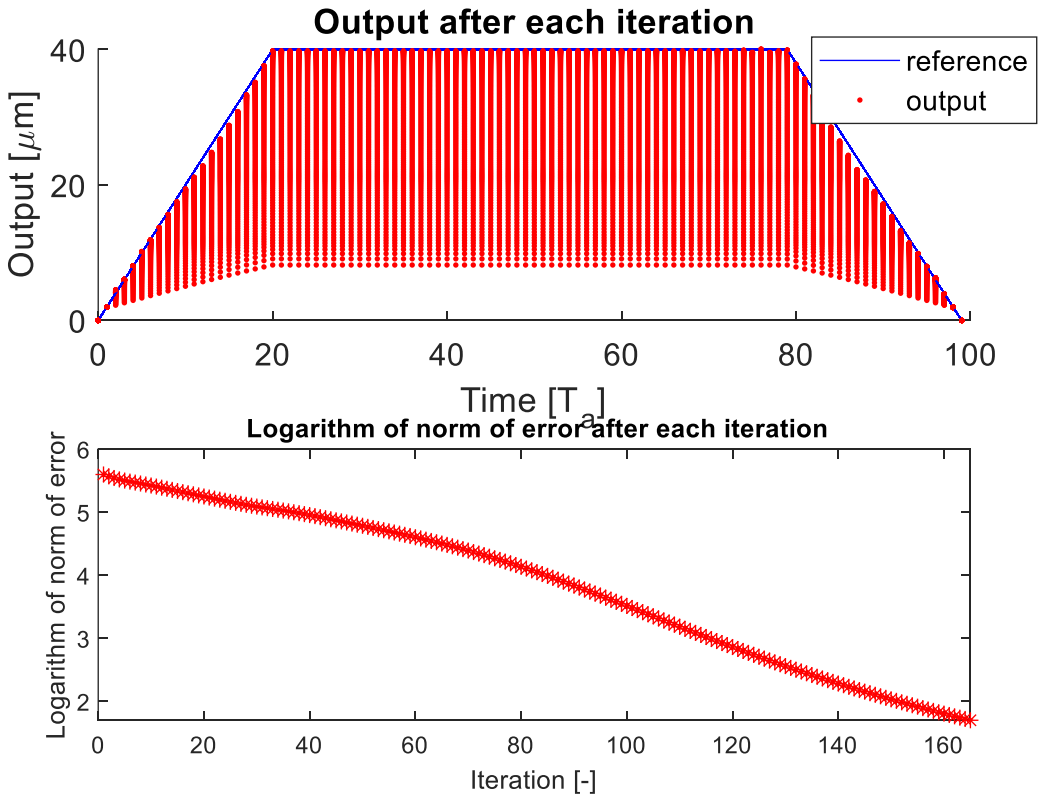

Fig. 5. Tracking error in dependence of learning number (PD-type)

For both learning algorithms, the output gradually converges to the reference value after a finite number of iterations, with the maximum steady-state error being around 0.23 μm (relative to the 40 μm reference amplitude). The PID learning algorithm achieves faster convergence and smaller

errors. To further reduce the error, the gains K_1, K_2, K_3 can be decreased; however, this would prolong the learning process.

Table 2. Material properties

Parameters	Symbol	Unit	Value
Density	d	kg/m^3	2330
Young's modulus	E	MPa	1.69×105
Thermal conductivity of air	k_a	W/m.K	0.0257
Specific heat	C_p	J/kg.K	712
Resistivity of silicon	ρ_0	Ω.m	148×10^{-6}
Heat transfer coefficient of silicon	λ	1/K	1.25×10^{-3}
Thermal conductivity	k_s	W/m.K	156
Thermal expansion coefficient	α_l	10^{-6} 1/K	2.62

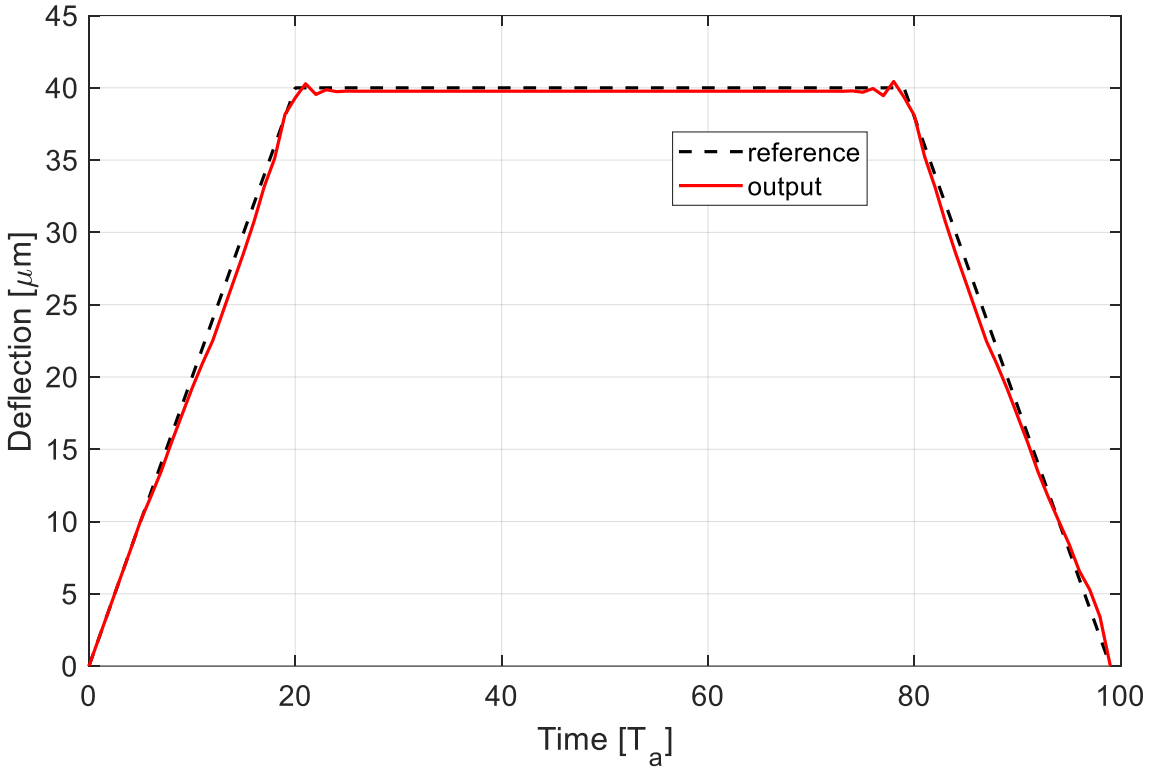

Fig. 6. Simulation results with a trapezoidal signal, after 165 iterations (PD-type)

The controller gainsK_P, K_I, K_Dwere selected based on prior experience and tuned to balance between convergence speed and steady-state accuracy. Larger errors mainly occurred at the rising and falling edges of the trapezoidal input (approximately 4.93% for PD and 4.33% for PID), while during the holding phase the error remained below 1%, which is acceptable for typical microgripper applications. Although parameter optimization could further refine performance for specific tasks, the current choice represents a reasonable trade-off between accuracy, simplicity, and computational efficiency. This also demonstrates that ILC, despite having a simpler structure compared to advanced controllers such as MPC or adaptive robust methods, remains effective and practical for MEMS implementation.

At this stage, the proposed work primarily focuses on theoretical modeling and simulation-based validation. Preliminary fabrication of the V-shaped microgripper with compliant rotary joints has been initiated using standard MEMS processes, but detailed experimental characterization (e.g., displacement calibration and stress analysis) is still in progress. These results will be presented in future work. Accordingly, the present manuscript mainly provides a foundation for model validation and controller design prior to full-scale experimental benchmarking.

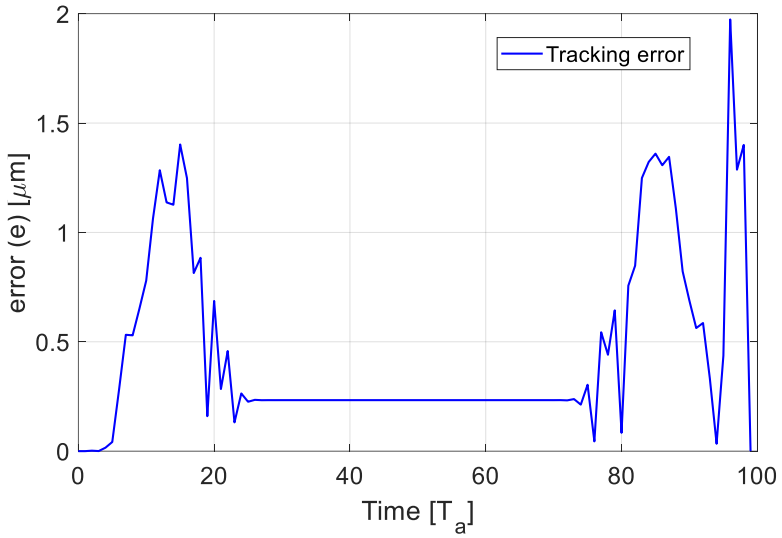

Fig. 7. Displacement error after 165 iterations (PD-type)

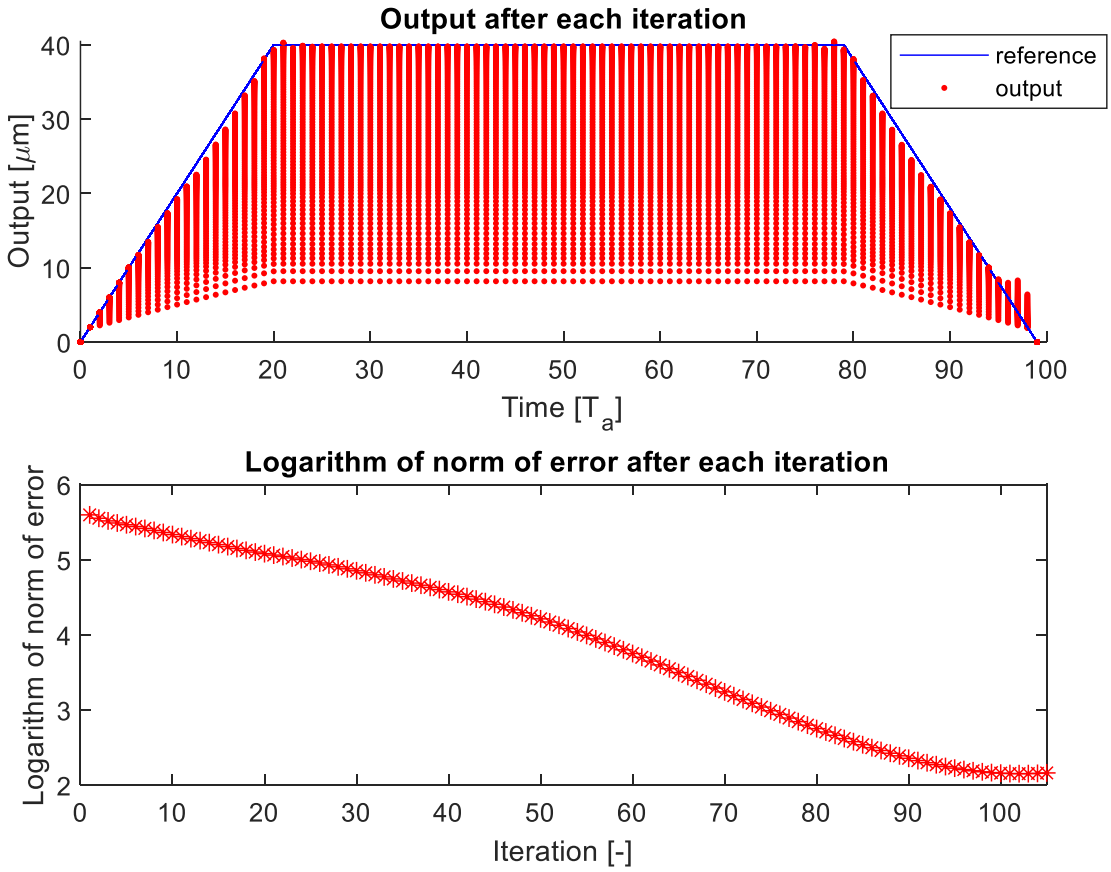

Fig. 8. Tracking error in dependence of learning number (PID-type)

It should also be noted that simplified modeling assumptions, together with unavoidable fabrication imperfections, may cause discrepancies between analytical predictions, simulations, and experimental outcomes. In similar MEMS processes, previous studies [61] have reported dimensional deviations of about (0.25–0.5)µm. For the current design, such deviations could lead to displacement errors of approximately (4.5–15)% compared to the ideal model prediction. This potential mismatch underlines the importance of accounting for fabrication tolerances during the design stage and further motivates our ongoing efforts toward experimental validation, robustness testing, and tolerance-aware controller tuning.

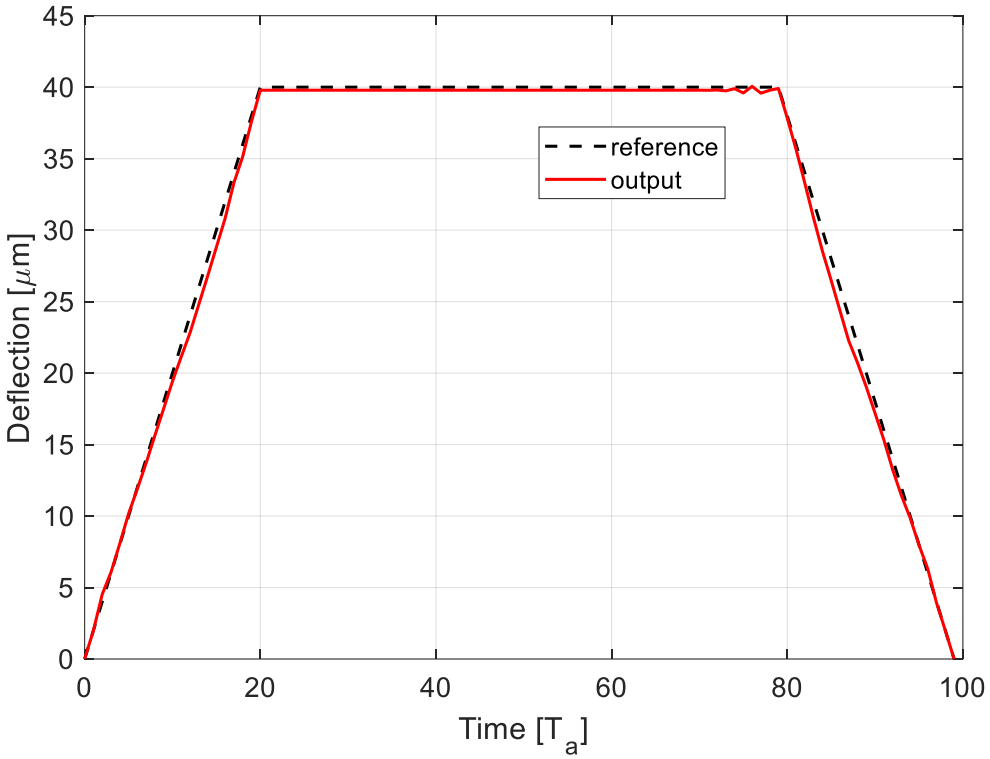

Fig. 9. Simulation results with a trapezoidal signal, after 105 iterations (PID-type)

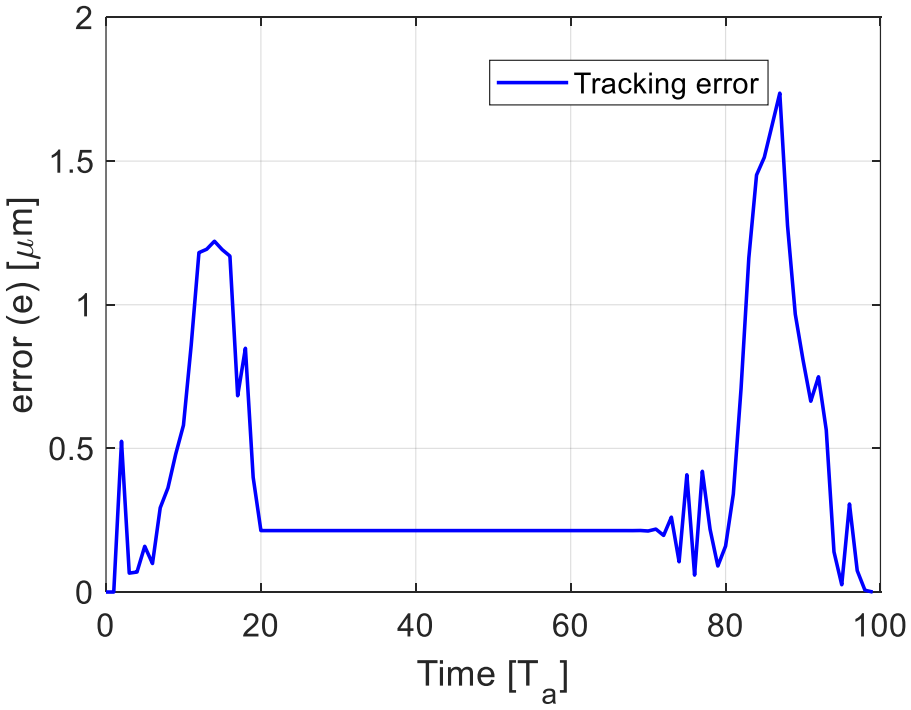

Fig. 10. Displacement error after 105 iterations (PID-type)

5. Conclusion

This work developed a comprehensive analytical model and control strategy for a V-shaped electrothermal microgripper with integrated compliant rotary joints. The model captured the coupled thermo–mechanical behavior of the actuator and the kinematic displacement amplification from the shuttle to the gripping jaws. By integrating iterative learning control (ILC) strategies, including PD-

ILC and PID-ILC, the study evaluated system performance in tracking a trapezoidal reference trajectory with a peak displacement of 40 µm.

Simulation results confirmed that both control methods achieved convergence within a finite number of iterations, with PID-ILC demonstrating superior performance in terms of convergence speed and tracking accuracy. Specifically, PID-ILC reduced the average sum of squared tracking errors (Norm) to 5.47 compared to 9.24 for PD-ILC, while maintaining a steady-state error of only 0.21 µm and a maximum post-convergence error of about 1.73 µm. These results emphasize the effectiveness of ILC in progressively reducing tracking errors over repeated cycles, while retaining a simple control structure well-suited for MEMS implementation.

The main contributions of this work include: (i) development of an analytically tractable yet accurate thermo–mechanical model for design and control synthesis; (ii) structural integration of compliant rotary joints that enhance displacement amplification and mitigate stress concentration; and (iii) quantitative evaluation of PD-ILC and PID-ILC for trajectory tracking of microgrippers. These contributions provide not only methodological value but also theoretical significance in modeling and control of MEMS electrothermal actuators.

Nevertheless, this study has some limitations. The results are currently limited to simulations without experimental validation. Simplified modeling assumptions (e.g., neglecting convection and assuming small angular deflections) may lead to discrepancies when compared with real prototypes. Furthermore, parameter sensitivity and fabrication tolerances may significantly influence performance.

Future research will concentrate on moving beyond simulations toward fabrication and experimental validation of prototype devices, thereby verifying the accuracy of the model and control strategies. Further efforts will focus on analyzing sensitivity and robustness under parameter variations and external disturbances, as well as exploring adaptive ILC schemes combined with feedforward compensation to mitigate transient errors. In addition, the proposed framework will be extended to more complex scenarios, such as multi-DOF micromanipulation or integration with vision-based feedback, aiming to broaden its applicability in biomedical handling, micro-assembly, and precision optics.

The practical significance of this research lies in demonstrating that a relatively simple yet systematic modeling and control framework can effectively support precise and repeatable micromanipulation. With experimental validation in future work, the proposed methodology has the potential for broad applications across high-tech fields where accuracy, reliability, and scalability are essential.

Author Contributions: Dzung Tien Nguyen led the research, developed the model, carried out simulations, and wrote the manuscript as the corresponding author. Duc Minh Ngo provided supervision, contributed to discussions, and revised the manuscript. Both authors approved the final version.

Acknowledgment: This research is supported by Thai Nguyen University of Technology under grant number T2024- TS18.

Conflicts of Interest: The authors declare no conflict of interest.

References

[1] H. Llewellyn-Evans, C. A. Griffiths, and A. Fahmy, "Microgripper design and evaluation for automated µ-wire assembly: A survey," *Microsystem Technologies*, vol. 26, no. 6, pp. 1745-1768, 2020, https://doi.org/10.1007/s00542-019-04741-4.

[2] A. T. Vidap, B. D. Deshmukh, and S. S. Pardeshi, "A review on compliant microgripper," Recent *Advances in Mechanical Engineering*, pp. 609-620, 2022, https://doi.org/10.1007/978-981-99-1894-2_52.

[3] Z. Samadikhoshkho, K. Zareinia and F. Janabi-Sharifi, "A Brief Review on Robotic Grippers Classifications," *2019 IEEE Canadian Conference of Electrical and Computer Engineering (CCECE)*, pp. 1-4, 2019, https://doi.org/10.1109/CCECE.2019.8861780.

[4] O. Darintsev, "Microgrippers: Principle of operation, construction, and control method," *Proceedings of 15th International Conference on Electromechanics and Robotics" Zavalishin's Readings"*, pp. 25-37, 2020, https://doi.org/10.1007/978-981-15-5580-0_2.

[5] S. Hussain, H. Elahi, H. Jabbar, A. Hamza, U. S. Khan, and M. M. Saleem, "An electrothermally actuated high amplification MEMS microgripper with integrated capacitive sensing for micromanipulation," *Sensors and Actuators A: Physical*, vol. 395, p. 117038, 2025, https://doi.org/10.1016/j.sna.2025.117038.

[6] Z. Guo, Z. Lyu and Q. Xu, "Design of a Piezoelectric-Driven Microgripper With Three Working Modes," *IEEE/ASME Transactions on Mechatronics*, vol. 29, no. 1, pp. 260-270, 2024, https://doi.org/10.1109/TMECH.2023.3276191.

[7] F. Wang, B. Shi, Z. Huo, Y. Tian, and D. Zhang, "Control and dynamic releasing method of a piezoelectric actuated microgripper," *Precision Engineering*, vol. 68, pp. 1–9, 2021, https://doi.org/10.1016/j.precisioneng.2020.10.014.

[8] T. K. Das, B. Shirinzadeh, M. Ghafarian, A. Al-Jodah, Y. Zhong, and J. Smith, "Design, analysis and experimental investigations of a high precision flexure-based microgripper for micro/nano manipulation," *Mechatronics*, vol. 69, p. 102396, 2020, https://doi.org/10.1016/j.mechatronics.2020.102396.

[9] P. L. Chang, I. T. Chi, N. D. K. Tran, and D. A. Wang, "Design and modeling of a compliant gripper with parallel movement of jaws," *Mechanism and Machine Theory*, vol. 152, p. 103942, 2020, https://doi.org/10.1016/j.mechmachtheory.2020.103942.

[10] Z. Lyu and Q. Xu, "Recent design and development of piezoelectric-actuated compliant microgrippers: A review," *Sensors and Actuators A: Physical*, vol. 331, p. 113002, 2021, https://doi.org/10.1016/j.sna.2021.113002.

[11] C. Liang *et al*., “Design and control of a novel asymmetrical piezoelectric actuated microgripper for micromanipulation,” *Sensors and Actuators A: Physical*, vol. 269, pp. 227-237, 2018, https://doi.org/10.1016/j.sna.2017.11.027.

[12] W. Chen, X. Zhang, H. Li, J. Wei, and S. Fatikow, "Nonlinear analysis and optimal design of a novel piezoelectric-driven compliant microgripper," *Mechanism and Machine Theory*, vol. 118, pp. 32-52, 2017, https://doi.org/10.1016/j.mechmachtheory.2017.07.011.

[13] Z. Lyu, Z. Wu, and Q. Xu, "Design and development of a novel piezoelectrically actuated asymmetrical flexible microgripper," *Mechanism and Machine Theory*, vol. 171, p. 104736, 2022, https://doi.org/10.1016/j.mechmachtheory.2022.104736.

[14] P. Wang and Q. Xu, "Design and modeling of constant-force mechanisms: A survey," *Mechanism and Machine Theory*, vol. 119, pp. 1-21, 2018, https://doi.org/10.1016/j.mechmachtheory.2017.08.017.

[15] C. Liang, F. Wang, Y. Tian, X. Zhao, and D. Zhang, "Development of a high speed and precision wire clamp with both position and force regulations," *Robotics and Computer-Integrated Manufacturing*, vol. 44, pp. 208-217, 2017, https://doi.org/10.1016/j.rcim.2016.09.006.

[16] S. Iqbal and A. Malik, "A review on MEMS-based micro displacement amplification mechanisms," *Sensors and Actuators A: Physical*, vol. 300, p. 111666, 2019, https://doi.org/10.1016/j.sna.2019.111666.

[17] K. T. Hoang, D. T. Nguyen, and P. H. Pham, "Impact of design parameters on working stability of the electrothermal V-shaped actuator," *Microsystem Technologies*, vol. 26, pp. 1479-1487, 2020, https://doi.org/10.1007/s00542-019-04682-y.

[18] K. T. Hoang and P. H. Pham, "Safe working condition and optimal dimension of the electrothermal V-shaped actuator," *Microsystem Technologies*, vol. 28, pp. 1673-1685, 2022, https://doi.org/10.1007/s00542-022-05309-5.

[19] D. T. Nguyen, P. H. Pham, and K. T. Hoang, "Improving displacement of silicon V-shaped electrothermal microactuator using platinum sputter deposition process," *Microelectronics International*, vol. 40, no. 4, pp. 239-245, 2023, https://doi.org/10.1108/MI-05-2022-0076.

[20] D. T. Nguyen, K. T. Hoang, and P. H. Pham, "Larger displacement of silicon electrothermal V-shaped actuator using surface sputtering process," *Microsystem Technologies*, vol. 27, pp. 1985-1991, 2021, https://doi.org/10.1007/s00542-020-04985-5.

[21] P. Shivhare, G. Uma, and M. Umapathy, "Design enhancement of a chevron electrothermally actuated microgripper for improved gripping performance," *Microsystem Technologies*, vol. 22, pp. 2623–2631, 2016, https://doi.org/10.1007/s00542-015-2561-0.

[22] M. M. Ali and S. Iqbal, "Design and analysis of novel microelectromechanical system based microgripper for manipulating microbiological species and micro objects," *Proceedings of the Institution of Mechanical Engineers, Part C: Journal of Mechanical Engineering Science*, vol. 238, no. 18, pp. 9107-9124, 2024, https://doi.org/10.1177/09544062241245545.

[23] M. Akbari, F. Barazandeh, and H. Barati, "A novel approach to design and fabricate an electrothermal microgripper for cell manipulation," *Sensors and Actuators A: Physical*, vol. 346, p. 113877, 2022, https://doi.org/10.1016/j.sna.2022.113877.

[24] P. H. Pham and D. Van Bui, "Single mask and low voltage of micro gripper driven by electrothermal V–shaped actuator," *Advances in Asian Mechanism and Machine Science*, pp. 593-600, 2022, https://doi.org/10.1007/978-3-030-91892-7_66.

[25] T. D. Phuc, P. H. Pham, K. T. Hoang, and N. T. Bui, "Nonlinear displacement of the electrothermal V-shaped actuator," *Shock and Vibration*, vol. 2024, p. 7121490, 2024, https://doi.org/10.1155/2024/7121490.

[26] N. T. Dzung, P. H. Phuc, N. Q. Dich, and N. D. Phuoc, "Iterative learning control for V-shaped electrothermal microactuator," *Electronics*, vol. 8, no. 12, p. 1410, 2019, https://doi.org/10.3390/electronics8121410.

[27] P. H. Pham, T. D. Nguyen, and K. T. Hoang, "Single mask and low voltage electrothermal micromotor," *Sensors and Actuators A: Physical*, vol. 374, p. 115481, 2024, https://doi.org/10.1016/j.sna.2024.115481.

[28] L. T. Anh, T. T. T. Nga, and V. V. Hoc, "PID-type iterative learning control for output tracking gearing transmission systems," *International Journal of Robotics and Control Systems*, vol. 1, no. 3, pp. 256-268, 2021, https://doi.org/10.31763/ijrcs.v1i3.395.

[29] D. T. T. Huyen, V. V. Hoc, and N. T. T. Hoa, "Proportional derivative-type iterative learning algorithm for a motion control system," *International Journal of Robotics and Control Systems*, vol. 3, no. 2, pp. 304-314, 2023, https://doi.org/10.31763/ijrcs.v3i2.975.

[30] M. Li, Z. Zhou, L. Yi, X. Wang, and S. Adnan, "Design of a test structure based on chevron-shaped thermal actuator for in-situ measurement of the fracture strength of MEMS thin films," *Nanotechnology and Precision Engineering*, vol. 2, no. 4, pp. 163-168, 2019, https://doi.org/10.1016/j.npe.2019.10.004.

[31] Y. Algoos, W. B. Lenz, F. Khan, and M. I. Younis, "An electrostatically actuated MEMS microgripper with high amplification for precision manipulation," *Sensors and Actuators A: Physical*, vol. 378, p. 115800, 2024, https://doi.org/10.1016/j.sna.2024.115800.

[32] H. Chen, X. J. Wang, J. Wang, and Z. W. Xi, "Analysis of the dynamic behavior of a V-shaped electrothermal microactuator," *Journal of Micromechanics and Microengineering*, vol. 30, no. 8, p. 085005, 2020, https://doi.org/10.1088/1361-6439/ab90cc.

[33] T. V. R. H. Vithanage, Y. W. R. Amarasinghe and W. A. D. M. Jayathilaka, "Design and Simulation of a Thermally Actuated Microgripper with a Compliant Bistable Release Mechanism for Biomanipulation," *2024 Moratuwa Engineering Research Conference (MERCon)*, pp. 139-144, 2024, https://doi.org/10.1109/MERCon63886.2024.10689058.

[34] Y. Dai, D. Li, and D. Wang, "Review on the Nonlinear Modeling of Hysteresis in Piezoelectric Ceramic Actuators," *Actuators*, vol. 12, no. 12, p. 442, 2023, https://doi.org/10.3390/act12120442.

[35] X. Guo *et al*., "Adaptive Dynamic Measurement, Trajectory Correction, and Error Evaluation Method in MEMS LiDAR System," *IEEE Transactions on Instrumentation and Measurement*, vol. 74, pp. 1-10, 2025, https://doi.org/10.1109/TIM.2025.3571085.

[36] B. Ding, X. Li, C. Li, Y. Li, and S. C. Chen, "A survey on the mechanical design for piezo-actuated compliant micro-positioning stages," *Review of Scientific Instruments*, vol. 94, no. 10, p. 101502, 2023, https://doi.org/10.1063/5.0162246.

[37] S. Kodera, T. Watanabe, Y. Yokoyama, and T. Hayakawa, "Microgripper Using Soft Microactuators for Manipulation of Living Cells," *Micromachines*, vol. 13, no. 5, p. 794, 2022, https://doi.org/10.3390/mi13050794.

[38] L. V. Pasaguayo, Z. Al Masry, S. Lescano, and N. Zerhouni, "Surgical microgrippers: a survey and analysis," *Journal of Medical Devices*, vol. 17, no. 3, p. 030801, 2023, https://doi.org/10.1115/1.4062950.

[39] F. Chen, Y. Gao, W. Dong and Z. Du, "Design and Control of a Passive Compliant Piezo-Actuated Micro-Gripper With Hybrid Flexure Hinges," *IEEE Transactions on Industrial Electronics*, vol. 68, no. 11, pp. 11168-11177, 2021, https://doi.org/10.1109/TIE.2020.3032921.

[40] Y. Chen *et al*., "Recent advances in field-controlled micro–nano manipulations and micro–nano robots," *Advanced Intelligent Systems*, vol. 4, no. 3, p. 2100116, 2022, https://doi.org/10.1002/aisy.202100116.

[41] A. A. Felix, D. Colón, B. M. Verona, L. W. Ramos, H. Cobas-Gomez, and M. R. Gongora-Rubio, "Identification and Robust Controllers for an Electrostatic Microgripper," *Journal of Vibration Engineering & Technologies*, vol. 9, no. 3, pp. 389–397, 2021, https://doi.org/10.1007/s42417-020-00241-2.

[42] Y. Hong, Y. Wu, S. Jin, D. Liu, and B. Chi, "Design and Analysis of a Microgripper with Three-Stage Amplification Mechanism for Micromanipulation," *Micromachines*, vol. 13, no. 3, p. 366, 2022, https://doi.org/10.3390/mi13030366.

[43] J. Cheng *et al*., "Recent Design and Application Advances in Micro-Electro-Mechanical System (MEMS) Electromagnetic Actuators," *Micromachines*, vol. 16, no. 6, p. 670, 2025, https://doi.org/10.3390/mi16060670.

[44] S. Darbasi, M. J. Mirzaei, A. M. Abazari, and G. Rezazadeh, "Adaptive under-actuated control for capacitive micro-machined ultrasonic transducer based on an accurate nonlinear modeling," *Nonlinear Dynamics*, vol. 108, pp. 2309-2322, 2022, https://doi.org/10.1007/s11071-022-07330-9.

[45] M. Macho, H. W. Yoo, R. Schroedter and G. Schitter, "Iterative Learning Control for Quasi-Static MEMS Mirror with Switching Operation," *2023 IEEE 36th International Conference on Micro Electro Mechanical Systems (MEMS)*, pp. 538-541, 2023, https://doi.org/10.1109/MEMS49605.2023.10052637.

[46] H. Zhu *et al*., "Selecting Robust Multi-Objective Optimization of a MEMS Electro-Thermal Actuator Considering Multi-Source Uncertainties," *IEEE Transactions on Electron Devices*, vol. 70, no. 7, pp. 3820-3827, 2023, https://doi.org/10.1109/TED.2023.3278621.

[47] X. Xu, P. Liu, S. Lu, F. Wang, J. Yang, and G. Xiao, "Iterative Learning with Adaptive Sliding Mode Control for Trajectory Tracking of Fast Tool Servo Systems," *Applied Sciences*, vol. 14, no. 9, p. 3586, 2024, https://doi.org/10.3390/app14093586.

[48] Z. Feng, J. Ling, M. Ming, and X. Xiao, "A model-data integrated iterative learning controller for flexible tracking with application to a piezo nanopositioner," *Transactions of the Institute of Measurement and Control*, vol. 40, no. 10, pp. 3201-3210, 2017, https://doi.org/10.1177/0142331217719958.

[49] H. Zhang, X. Fu, S. Liu and Y. Wang, "Iterative Learning Embedded Composite Model Reference Adaptive Control for Off-Axis In-Situ Rotation in Nanorobotic Manipulation," *IEEE Control Systems Letters*, vol. 8, pp. 291-296, 2024, https://doi.org/10.1109/LCSYS.2023.3336545.

[50] N. L. Ho, T. P. Dao, N. Le Chau, and T. M. Hoang, "Multi-objective optimization design of a compliant microgripper based on hybrid teaching learning-based optimization algorithm," *Microsystem Technologies*, vol. 25, pp. 2067-2083, 2019, https://doi.org/10.1007/s00542-018-4222-6.

[51] Y. Zhang and Q. Xu, "Variable structure control combined with adaptive iterative learning control for motion tracking of a piezoelectric microgripper," *2016 IEEE International Conference on Robotics and Biomimetics (ROBIO)*, pp. 1548-1553, 2016, https://doi.org/10.1109/ROBIO.2016.7866547.

[52] S. Riaz, R. Qi, O. Tutsoy, and J. Iqbal, "A novel adaptive PD-type iterative learning control of the PMSM servo system with the friction uncertainty in low speeds," *PloS one*, vol. 18, no. 1, p. e0279253, 2023, https://doi.org/10.1371/journal.pone.0279253.

[53] M. Macho, “Precision learning control for quasisStatic MEMS mirrors,” *Diploma Thesis, Technische Universität Wien*, 2023, https://doi.org/10.34726/hss.2023.96840.

[54] S. Sharma, S. Nabavi, A. A. S. Rabih, M. Ménard and F. Nabki, "Hybrid MEMS Actuator With 3 Degrees-of- Freedom for Efficient Planar Optical Switching," *Journal of Microelectromechanical Systems*, vol. 32, no. 6, pp. 593-603, 2023, https://doi.org/10.1109/JMEMS.2023.3322223.

[55] Y. Yu, C. Zhang, X. Zhang, C. -Y. Su and M. Zhou, "Iterative Learning Control Based on Neural Network and Its Application to Ni-Mn-Ga Alloy Actuator With Local Lipschitz Nonlinearity," *IEEE Transactions on Industrial Informatics*, vol. 20, no. 6, pp. 8138-8148, 2024, https://doi.org/10.1109/TII.2024.3369229.

[56] W. Ting and S. Aiguo, "An adaptive iterative learning based impedance control for robot-aided upper-limb passive rehabilitation," *Frontiers in Robotics and AI*, vol. 6, p. 41, 2019, https://doi.org/10.3389/frobt.2019.00041.

[57] D. Wang, Y. Zhao, H. Yang, and K. Hong, "Closed-loop control of microgripper system based on compliant mechanism," *AIP Advances*, vol. 14, no. 7, p. 075227, 2024, https://doi.org/10.1063/5.0206315.

[58] A. Potekhina and C. Wang, "Review of Electrothermal Actuators and Applications," *Actuators*, vol. 8, no. 4, p. 69, 2019, https://doi.org/10.3390/act8040069.

[59] C. -C. Huang, H. -C. Chen, K. -W. Huang and L. -C. Fu, "Iterative Learning Controller with Learning Gain Optimization and Online Data Adjustment for Atomic Force Microscope," *2020 International Automatic Control Conference (CACS)*, pp. 1-6, 2020, https://doi.org/10.1109/CACS50047.2020.9289760.

[60] P. D. Pour, M. Ghommem, and A. Abdelkefi, "Modeling and Design Enhancement of Electrothermal Actuators for Micrograpping Applications," *Applied Sciences*, vol. 13, no. 18, p. 10140, 2023, https://doi.org/10.3390/app131810140.

[61] P. H. Pham and L. B. Dang, "Influence of the side etching effect in DRIE on performance of electrostatic linear comb-drive actuators," *Microsystem Technologies*, vol. 24, pp. 2215-2222, 2018, https://doi.org/10.1007/s00542-017-3685-1.